16th World Conference on Earthquake, 16WCEE 2017
Santiago Chile, January 9th to 13th 2017
Paper N° 4495
Registration Code: S-R1464692017

SITE RESPONSE EVALUATION IN A VOLCANIC AREA USING H/V AND 1D WAVE PROPAGATION ANALYSIS

G.Ö. Sigurðsson[(1)], R. Rupakhety[(2)], S. Ólafsson[(3)]

[(1)] *Research Scientist, Earthquake Engineering Research Centre, University of Iceland, gos12@hi.is*
[(2)] *Professor, Earthquake Engineering Research Centre, University of Iceland, rajesh@hi.is*
[(3)] *Research Professor, Earthquake Engineering Research Centre, University of Iceland, simon@hi.is*

Abstract

This contribution presents some results of a detailed site response analysis in a proposed wind farm site in South Iceland. The area under study is a valley Northwest of Mount Hekla in South Iceland, and the sites consist of layers of soft sand mixed with scoria/tephra sandwiched between layers of very stiff basalt. The analysis is based on Horizontal to Vertical Spectral Ratios (HVSR) of ambient vibrations as well as one dimensional equivalent linear wave propagation analysis. Wave propagation analysis, also known as site response analysis, is based on geotechnical data from the study area, mostly in the form of borehole logs. Fundamental site vibration frequencies obtained from HVSR and site response analysis were found to be consistent throughout the study area. Site fundamental frequencies inferred from average shear wave velocity in the upper 30m of the sites were found to be significantly larger—4 times on the average—than those inferred from elastic transfer functions. The response of the sites under several pulse-like and ordinary ground motions was computed. The results indicate that inelastic deformations of the soft layers cause reduction in fundamental frequencies of the sites and the corresponding amplification factors. This reduction was found to be strongly correlated with peak ground velocity of pulse-like ground motions and peak ground acceleration of ordinary ground motions.

Keywords: Site-response analysis; HVSR; Ambient vibrations; Seismic ground motion; Site amplification

1. Introduction

The National Power Company of Iceland, Landsvirkjun, is planning to construct a wind farm in the Búrfellslundur area in South Iceland (see Fig. 1). Since the proposed wind farm lies in the close vicinity of the South Iceland Seismic Zone, detailed investigation of seismic hazard at the site is necessary. An important aspect of this investigation is the quantification of effects of local geology, commonly known as local site effects, in the ground motion at the surface. Depending on the geotechnical properties of the site, ground motion amplitudes at certain frequencies may be amplified (in comparison to that at outcropping bedrock) while those at other frequencies may be reduced. The proposed site is a lava field east of mount Búrfell. The local geology at Búrfellslundur area consists of layers of basalt with some layers of soft sediments and tephra/scoria sandwiched between them.

2. The study area

The study area lies in South Iceland, near the north-eastern edge of the South Iceland Seismic Zone. This zone is one of the most seismically active areas in Iceland where many earthquakes have occurred in the past. The geographical location of the study area is shown in a map of Iceland in Fig. 1. Two alternative areas are under consideration for the construction of a wind farm as is explained in [1]. Based on borehole logs as well as other relevant data, a schematic cross section of the study area has been prepared by Ingólfsson [1]. The locations where stratigraphic profiles are available are shown in Fig.2a. The area is built up on massive lava flows which are separated by thick layers of tephra and sand. A typical geological profile in the study area consists of several basalt layers, each with a scoria crust on top and tephra layers in between (see Fig.2b). At some locations, fluvial sediments are mixed with tephra. The most detailed stratigraphic information of the study area is available in the form of core-drilling borehole logs [1] at three locations in the proposed area. The three boreholes are BFC-2, BFC-3, and BFC-4 (see Fig. 2a). In addition, two logs obtained from percussion-drilled holes (BFP-2 and BFP-3, see Fig. 2a) are also available. A number of publicly available reports describe properties of geotechnical materials in Iceland (see, for example, [2]). Estimates of the mechanical properties of rock layers in the study area were also provided by Ingólfsson [3] on behalf of EFLA Consulting Engineers. The properties estimated by Ingólfsson [3] were found to be consistent with those reported in published reports, and are used for further analysis. These properties are listed in Table 1.

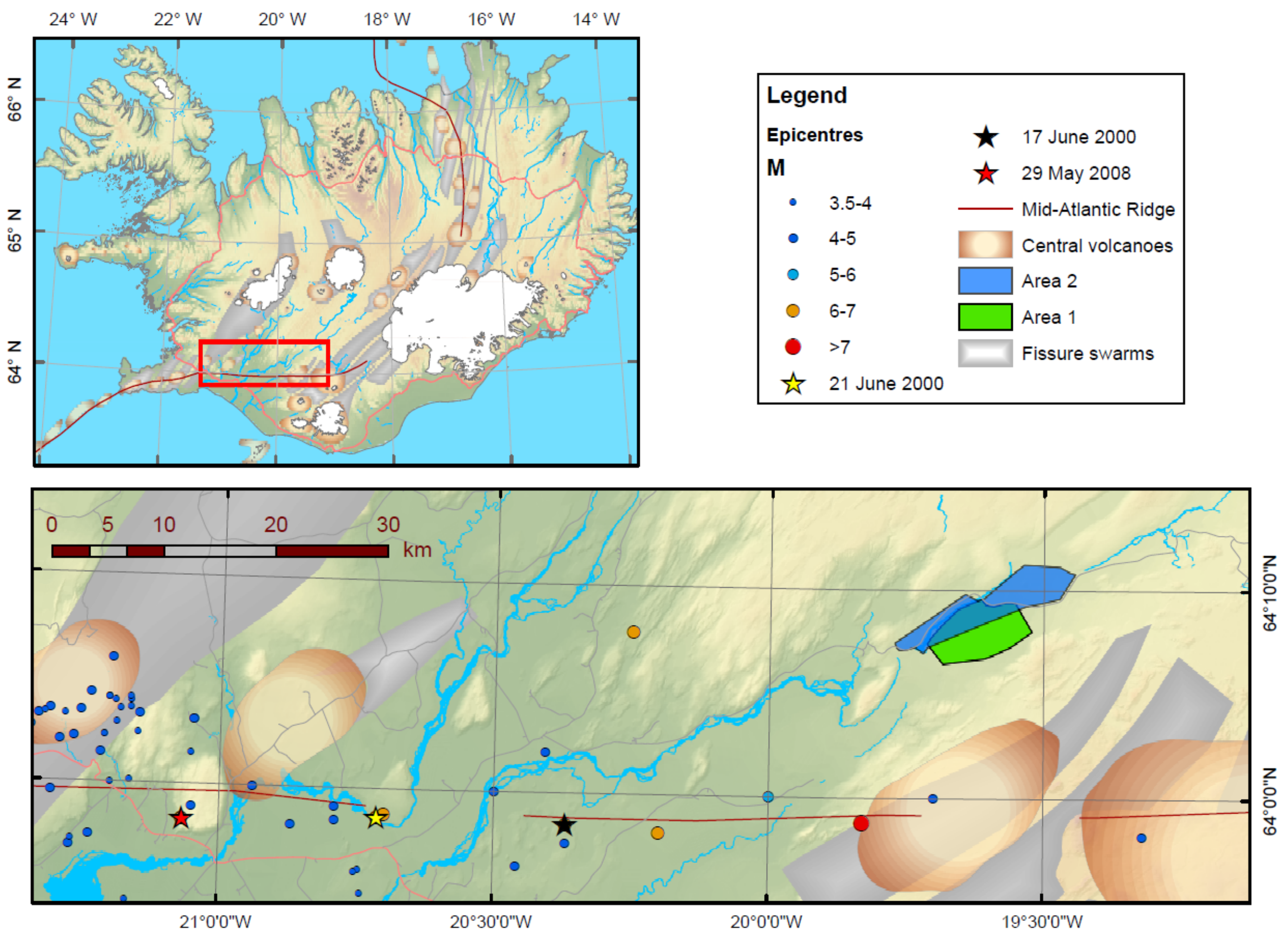

Fig. 1 – Top-left: Map of Iceland showing main geological features. Bottom: Enlarged view of the area indicated by the red-rectangle on the map on top-left. The two alternative areas (see, [1]) proposed for the windfarm are indicated by the blue and the green polygons. The epicentres of earthquakes recorded in the area are shown with the circles; the three stars indicate the epicentres of the June 2000 and May 2008 earthquakes as explained in the legend.

2. HVSR method

The HVSR method is a widely used method for site effects characterization, especially for estimating the predominant frequency of the site. The method was originally proposed by Nogoshi and Igarashi [4] but was popularized by Nakamura who described it in a highly quoted paper [5], and as a result it is often referred to as the Nakamura method. In this study we use the HVSR method on ambient vibrations recorded at several sites in the study area. The locations where such recordings were made are indicated by the triangles in Fig. 2a. The ambient vibration measurements were performed during the period of June to October 2015. The guidelines from the SESAME project [6] were used as a reference for performing the measurements. The instruments used for the measurements were a Lennarz LE-3D/5s velocity sensor and Obsidian 24-bit data acquisition unit from Kinemetrics Inc. The main emphasis was on measuring at the locations of the deepest and the most recently drilled boreholes (BFC-2, BFC-3, BFC-4, BFP-2, BFP-3, LD-9). Measurement was also made at the location of a few other boreholes (PH-93, ST-7, TH-4) that were further to the north-east, closer to Sultartangi Dam, and also some of the sites of the ram sounding boreholes (HC-3, HC-6, HC-8, HC-13, HC-25, HC-28, HC-28, HC-40, HC-43, HC-57).

The HVSR curves were calculated using Geopsy, which is an open source software for geophysical research and application written during the SESAME project (www.geopsy.org). In most cases, 40s windows were used for HVSR estimation. An automated process using the short time average (STA) over long time average (LTA) was used for selecting the windows from 40-minute records so that transients were effectively discarded. A mean HVSR curve was then obtained from the selected windows and then further smoothed using the filter named after Konno-Ohmachi [7]. A smoothing constant of 20 was used with a 5% cosine taper at the ends. The horizontal spectrum was obtained by squared averaging of two orthogonal horizontal components.

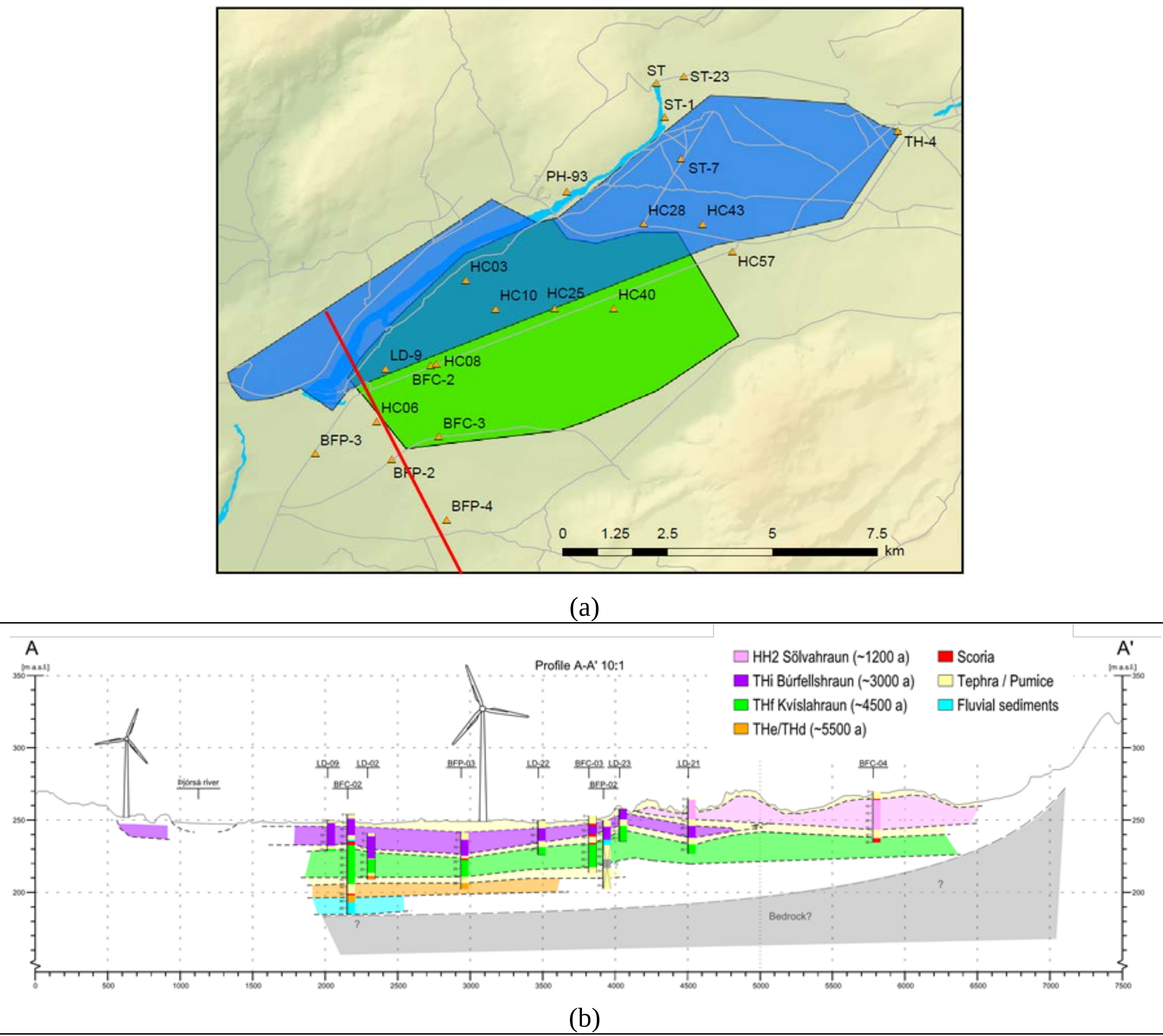

Fig. 2 – (a): The two alternative areas proposed for wind farm construction (see also Fig. 1). The triangles indicate the locations where geotechnical site profiles are available. (b): A schematic geological profile of the area. The orientation and location of the profile is indicated by the red line in Fig. 2a. The profile was created by Ingólfsson [1]. The colors indicate the different geotechnical materials as indicated in the legend; the four items in the first column of the legend represent different types of basalt, and their approximate age are as indicated in the parenthesis.

Table 1 – Mechanical properties of geotechnical materials found in the study area.

Material	**Density (kg/m³)**	**Poisson's ratio**	**Young's modulus (GPa)**
Basalt (Búrfells)	2840	0.23	27.00
Basalt (Kvíslar)	2830	0.23	27.00
Basalt	2790	0.23	27.00
Tephra with lava blocks	1900	0.25	0.43
Tephra with sand	1900	0.25	0.43
Scoria	2450	0.20	8.00

3. Wave propagation analysis

The methodology used in one-dimensional site response analysis can be easily formulated for a harmonic shear wave travelling vertically. The profile is divided into a number of layers based on local geotechnical information (see Fig. 3b). Each layer m is characterized by a certain thickness h_m. The bedrock is modelled as an elastic half space. The mechanical (constitutive) behaviour of each layer is approximated by a Kelvin-Voigt solid:

$$\tau = G\gamma + \eta\dot{\gamma} \tag{1}$$

where τ is the shear stress, G is the shear modulus, η is viscosity, γ is shear strain, and $\dot{\gamma}$ is strain rate. For harmonic motion with angular frequency ω, the displacement can be represented as:

$$u(z,t) = U(z)e^{i\omega t} = \left(Ee^{ik^*z} + Fe^{-ik^*z}\right)e^{i\omega t} \tag{2}$$

where $U(z)$ is the depth-dependent amplitude of harmonic motion, t denotes time, and i represents imaginary unit. Here $k^* = \omega\sqrt{\rho / G^*}$ is the complex wave number, ρ is mass density; $G^* = G(1+2i\xi)$ is the complex shear modulus with $\xi = \omega\eta / 2G$ as the damping ratio expressed as a percentage of critical damping. The amplitudes of waves in layer m (E_m and F_m) can be related to the amplitudes in layer $m+1$, through the following equations.

$$E_{m+1} = \frac{E_m\left(1+\alpha_m^*\right)e^{ik_m^*h_m}}{2} + \frac{F_m\left(1-\alpha_m^*\right)e^{-ik_m^*h_m}}{2} \tag{3}$$

$$F_{m+1} = \frac{E_m\left(1-\alpha_m^*\right)e^{ik_m^*h_m}}{2} + \frac{F_m\left(1+\alpha_m^*\right)e^{-ik_m^*h_m}}{2} \tag{4}$$

where α_m^* is the complex impedance ratio between the layers and is defined by the following equation.

$$\alpha_m^* = \sqrt{\frac{\rho_m G_m^*}{\rho_{m+1} G_{m+1}^*}} \tag{5}$$

Equations 3 and 4 describe how a wave amplitude is modified when it propagates from one layer to another. The transfer function relating the displacements at the top of layers m and n can be defined as the ratio between the amplitudes of motion as :

$$H_{mn}(\omega) = \frac{E_m + F_m}{E_n + F_n} \tag{6}$$

By applying Eq. 3 and 4 successively from the top layer to the bottom layer, the transfer function of the whole profile can be computed. In order to apply these equations recursively, the stress-free condition at the free surface is invoked which results in $E_1 = F_1$. The transfer function is complex, and its modulus is commonly known as the gain or amplification function. When the bedrock outcrops, the amplitude of upcoming and down-going waves at the outcropping surface must be able equal. On the other hand, this not the case within the bedrock, for example at the bottom of the profile (see Fig. 3a). To account for this effect, the modified transfer function given by Eq. 7 is used in all further analysis.

$$H_{mn}(\omega) = \left(\frac{E_n + F_n}{2E_n}\right)\left(\frac{E_m + F_m}{E_n + F_n}\right) = \left(\frac{E_m + F_m}{2E_n}\right) \tag{7}$$

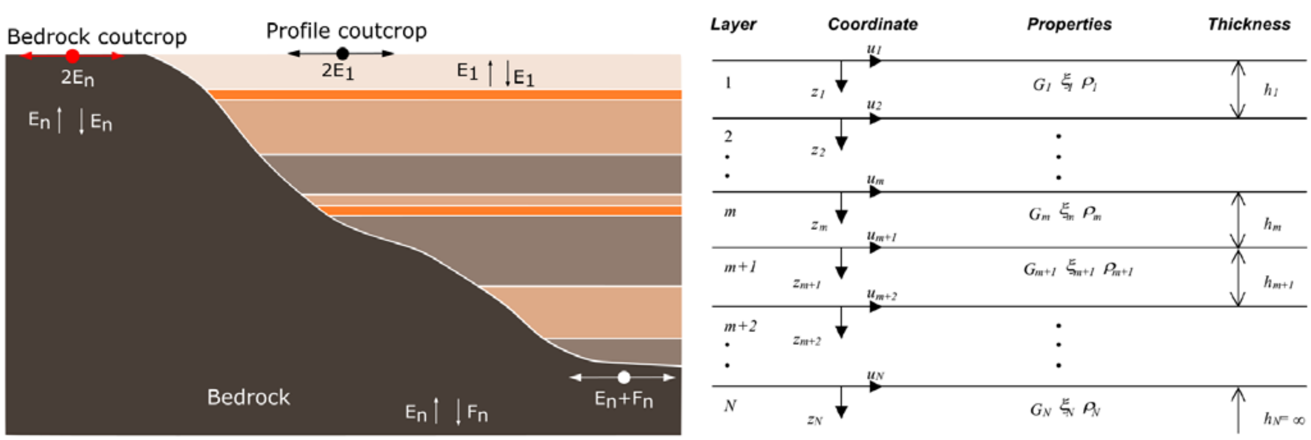

Fig. 3 - a) Schematic illustration of surface motion, inside bedrock motion, and bedrock outcropping motion. b) One-dimensional modelling of a layered soil deposit (from [8])

By virtue of the Fourier Theorem, and periodic approximation, frequency domain analysis using Fourier Transformation can be used to compute transient response of a profile. If $U(\omega)$, $Y(\omega)$, and $H(\omega)$ denote the Fourier Transform of ground acceleration at outcropping bedrock, Fourier Transform of ground acceleration at the surface of the profile, and transfer function of the profile, respectively; the following equation holds.

$$Y(\omega) = U(\omega)H(\omega) \tag{8}$$

Once $Y(\omega)$ is computed, ground acceleration at the surface of the profile is obtained by calculating its discrete inverse Fourier Transform. In this manner, the response of the soil profile to any arbitrary excitation can be obtained. The computational method discussed above is valid only for linearly elastic system. This is due to the fact that the frequency domain operation represented by Eq. 7 is equivalent to a convolution operation in time domain, which is a valid method of solution only when the system being analysed is linearly elastic. To model inelastic (non-linear) effects, equivalent linear site response analysis can be used. The analysis relies on a search for a linear model, which is, in a broad sense, equivalent to the actual non-linear system. This process is called equivalent linearization. The equivalent linear system is expected to be softer than a purely elastic system which implies reduction in shear modulus. Furthermore, hysteretic behaviour during non-linear deformation dissipates energy, which results in increase of damping ratio. As the effective reduction in modulus or increase in damping is to be modelled as an average phenomenon rather than that corresponding to the maximum strain (which may be imposed only for a short duration of time), inelastic effects need to be quantified in terms of some kind of average strain rather than the maximum strain. Such a strain is known as the effective strain and is a fraction of the maximum strain:

$$\gamma_{eff} = R\gamma_{\max} \tag{9}$$

where $\gamma_{\max}$ is the maximum strain and R is a reduction factor which has been found to be dependent, in case of earthquake excitation, on the moment magnitude (M).

The dependence of shear modulus and damping ratio on effective strain for different soil/rock types have been reported in the literature (see, for example, [9]). For simplicity, relationship between effective strain and shear modulus or damping ratio are called as material curves hereafter. For the basalt layers, material curves corresponding to rock as proposed by [10] are used. The softer layers which contain sand and tephra have been found to behave differently than alluvial sand (see, for example, [11]). From a detailed survey of the literature (including [11]), it was concluded that the shear modulus reduction curve for volcanic sand lies approximately between sand and clay models proposed by [10]. The material curves adopted in this study are shown in Fig. 4.

In general, transfer functions are only defined for linearly elastic system. As the material goes into inelastic phase, its stiffness and damping properties change with the level of excitation, and a unique transfer function is not defined. In the framework of equivalent linear system, however, an equivalent linear transfer function can be defined based on the properties of the equivalent linear system.

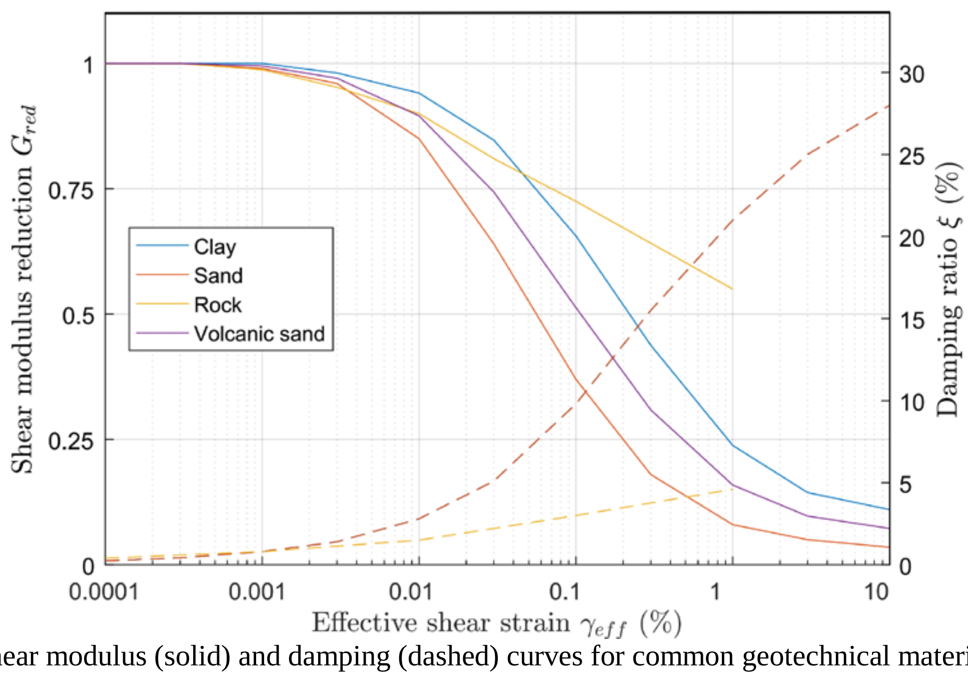

Fig. 4 - The shear modulus (solid) and damping (dashed) curves for common geotechnical materials (the sand, clay, and rock models are as reported in [9]). The shear modulus reduction curve of volcanic sand (mixture of sand and tephra/scoria) is assumed to be the average of that of clay and sand.

4. Linear (Elastic) transfer function

The elastic transfer function of a site provides information about the elastic vibration frequencies of the site. This transfer function is relevant when ground motions are small enough so that the soil layers remain elastic. For elastic modelling, the shear modulus remains unchanged at initial elastic value as does the critical damping ratio. Elastic transfer functions were computed at several sites in the study area. As HVSR are typically estimated from weak ambient vibrations, they represent elastic behaviour of the site. In this sense, the peaks of HVSR and elastic transfer functions are expected to occur at similar frequencies provided that the transfer functions are derived from a reliable model of the actual site condition.

Comparison between HVSR and the modulus of the elastic transfer function (amplification) at BFC-2 and BFP-2 is presented in Fig. 5. The results indicate that the fundamental site frequency inferred from HVSR and elastic amplification functions are similar. In general, the similarity was found to be the strongest at the deepest boreholes, as expected. However, there were considerable differences in the higher mode frequencies as well as amplification factors. Nevertheless, the higher mode frequencies (around 6 Hz) are not relevant for the structures being considered which are expected to have a fundamental frequency around 0.3 Hz [12]. At shallower boreholes, frequencies of peaks inferred from HVSR differed somewhat from those inferred from elastic amplification functions. Upon extrapolation of these profiles based on neighbouring boreholes (and the profile shown in Fig. 2b), the frequencies matched better. This shows that, although HVSR method may not yield complete information on the dynamic characteristics (especially the amplification factors), it can be used to supplement available geotechnical information for site response analysis.

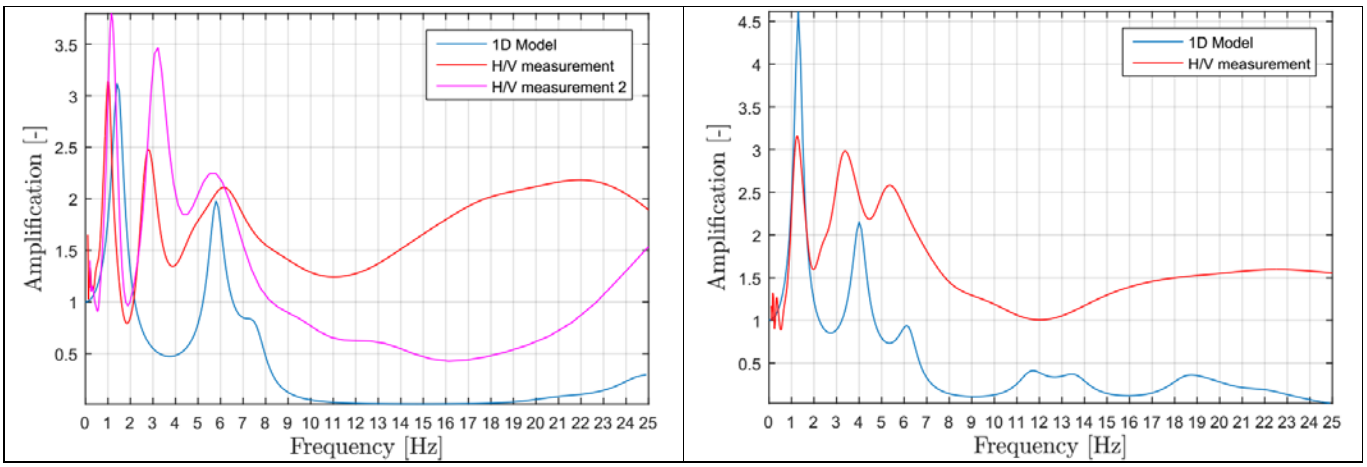

Fig. 5 - Comparison of HVSR with elastic amplification function (shown in blue) at station BFC-2 (left) and BFP-2 (right).

5. Equivalent linear transfer function

This section reports and discusses the transfer function of the sites being studied when they are loaded beyond their elastic limit. As discussed earlier, inelastic behaviour is excitation dependent. To account for this dependence, a number of recorded earthquake ground motions were used as excitation. The selection of these excitations was made to represent expected seismic scenarios in the study area. Inelastic transfer functions of the site when excited by pulse-like and non-pulse-like ground motions are studied separately to investigate potential effects of long-period pulse-like ground motions. Pulse-like ground motions from a database complied and processed by Rupakhety [13] are considered as candidate ground motions for this study. To comply with expected scenarios at the proposed site, only those earthquakes with strike-slip source mechanism and having a moment magnitude larger than 5.5 are considered. In total, 46 records fulfil the stated criteria and are used for site amplification analysis. Non-pulse-like records were selected from the internet site for European strong-motion data [14]. Only those ground motions with source-site distance larger than 30 km were selected to avoid ground-motions with potential near-source effects. Further details on the selection and scaling of ground-motions are provided in [15]. In total, 23 non-pulse-like ground motions with PGA in the range 0.2-0.45g were used.

Amplification curves (modulus of equivalent linear transfer functions) corresponding to the pulse-like and non-pulse-like ground motions are shown in Fig. 6. It can be noticed that the frequency and amplitude of the peaks of the amplification curves vary from one ground motion to another. The average amplification curves are shown in black in Fig. 6. The amplitudes of the peaks seem to be more sensitive to ground motion characteristics than the frequencies. It can be noticed that the frequencies of peaks are slightly reduced compared to the elastic transfer function. The mean amplification curves of non-pulse-like ground motions appear, at first sight, similar to that of pulse-like ground motions. In terms of frequencies of the peaks, the results are quite similar. This is expected because as long as the amplitude of excitation is consistent, the frequency of vibration of the site should depend more on the properties of the site than frequency content of ground motion. On closer comparison, however, it can be noticed that non-pulse-like ground motions amplify higher frequencies more while pulse-like ground motions amplify lower frequencies more.

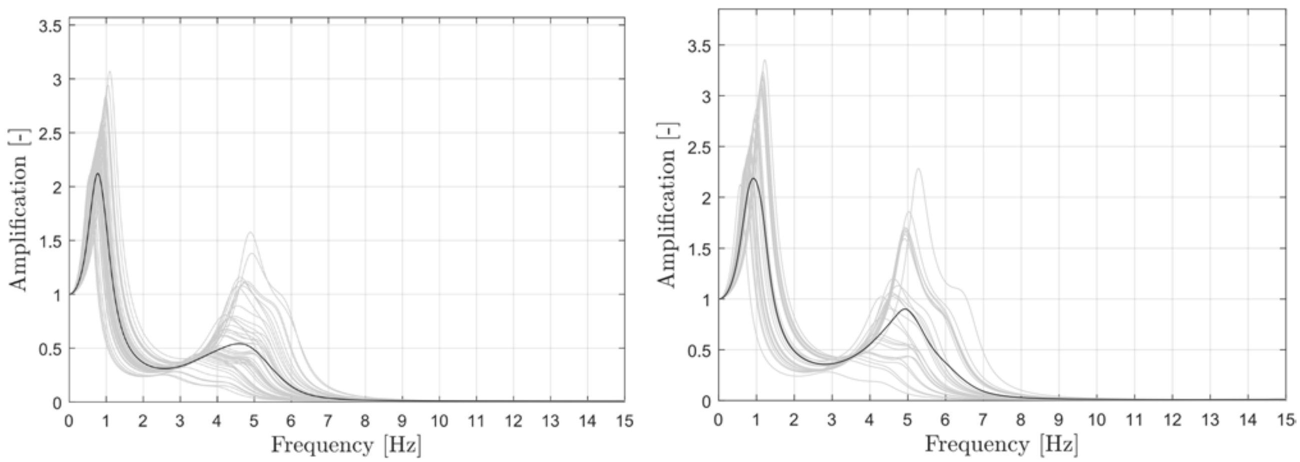

Fig. 6 - Amplification curves at BFC-2 corresponding to 46 pulse-like ground motions (left) and 23 non-pulse-like ground motion(right), shown in grey. The black curves represent mean (across the ground motions) amplification.

The variation of site fundamental frequency and the corresponding amplification with amplitude (selected as peak ground velocity, PGV) of pulse-like ground motions is shown in Fig. 7. It can be noticed that the site frequency and the corresponding amplification decrease considerably with increasing ground-motion amplitude. With stronger excitation, higher strains are induced in the geotechnical materials, resulting in lower shear modulus and higher damping ratio. Reduction in shear modulus results in lower fundamental site frequency, while increase in damping lowers the corresponding amplification. For non-pulse like ground motions, a similar trend can be observed (see Fig. 8) in terms of peak ground acceleration (PGA). The effect of ground-motion amplitude in site fundamental frequency and the corresponding amplification factor seems to be more pronounced for pulse-like ground motions than non-pulse-like ground motions. On the other hand, amplitudes of non-pulse-like ground motions seem to have more impact at higer frequencies.

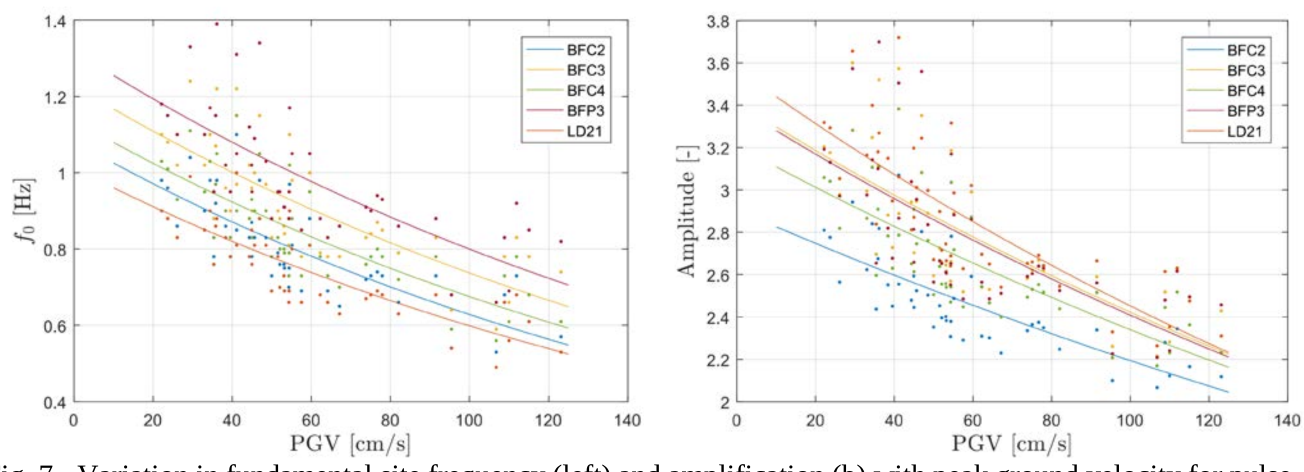

Fig. 7 - Variation in fundamental site frequency (left) and amplification (b) with peak ground velocity for pulse-like motion at five different stations in the study area. The dots represent results from various ground motions, and the solid lines represent exponential models fitted to the results.

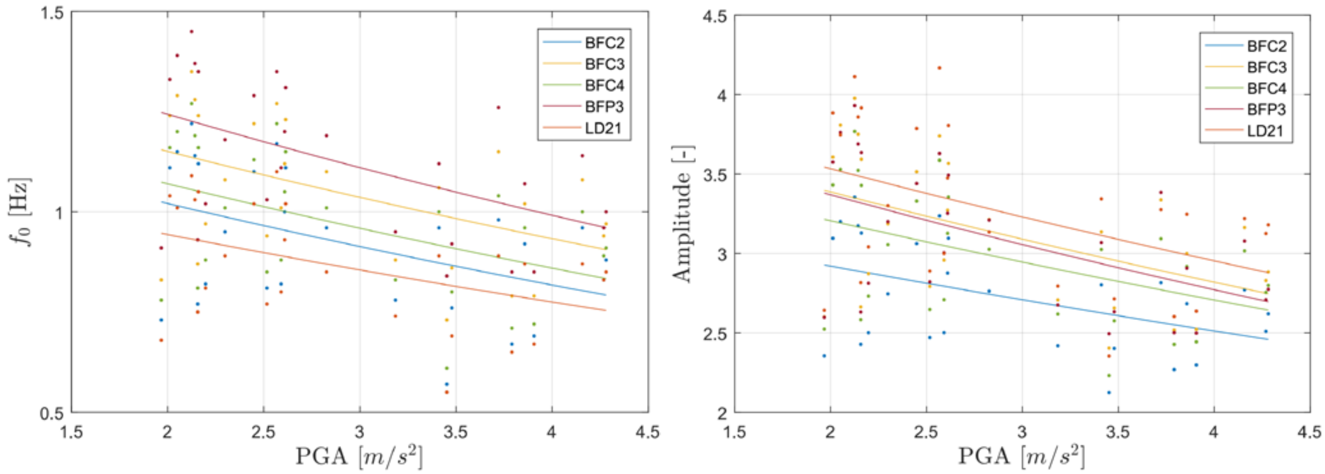

Fig. 8 - Variation of fundamental site frequency (a) and amplification (b) with amplitude of non-pulse-like ground-motions.

6. Average shear wave velocity as a site parameter

In various earthquake design codes, for example Eurocode 8 [16] and UBC [17], the average velocity of shear waves in the top 30m of the earth layers is used as an indicator of site class. The average velocity of shear waves in the top 30m of the surface layers, $V_{S,30}$, can be computed as follows:

$$V_{S,30} = \frac{\sum_{i=1}^{n} h_i}{\sum_{i=1}^{n} \frac{h_i}{V_i}} \tag{10}$$

where n is the number of layers, h_i is the thickness of layer i and V_i is the S-wave velocity in the layer. For $V_{S,30}$ the total thickness of the layers is 30m, i.e. the numerator in Eq. 10 is 30m. This parameter is also widely used in ground motion prediction equations (GMPEs) to represent local site effects. It is also a common practice to estimate site fundamental frequency based on $V_{S,30}$. In some applications, site fundamental frequency obtained from HVSR analysis are used to estimate $V_{S,30}$. The suitability of using $V_{S,30}$ to estimate fundamental site frequency was tested in this study. The test comprises of comparing fundamental site frequency obtained by using $V_{S,30,}$ hereafter denoted as F_{30}; with that obtained from HVSR, hereafter denoted as, F_0; and that obtained from elastic as well as equivalent elastic transfer functions, hereafter denoted as F_e and F_i, respectively. The estimation of fundamental frequencies from HVSR curves are described in more detail in [15]. These frequencies are listed in Table 2 for 7 different sites in the study area. The frequency corresponding to equivalent elastic transfer function is obtained from the average transfer function of the sites when subjected to all the ground motion used in this study.

The comparison in Table 2 shows that the fundamental frequencies obtained from HVSR and elastic transfer function are similar, with the former being about 25% smaller than the latter on the average. The comparison is presented graphically in Fig. 9. The frequencies inferred from equivalent elastic transfer functions are, on the average, about 40% smaller than those inferred from elastic transfer functions.

The frequencies obtained from $V_{S,30}$ are much higher; about 4 times larger than those inferred from elastic transfer function, on the average. This observation indicates that $V_{S,30}$ is not a good indicator of site characteristics in the study area. The reason that average shear wave velocity does not represent the actual behaviour of the sites being studied is that it is not able to model discontinuities (sharp impedance contrasts) between the stiff rock and soft tephra/scoria layers at the sites. The vibration frequencies and mode shapes of sites with very soft layers sandwiched between very stiff rocks is controlled by the stiffness of the soft layers. In more general term, the site may be considered to behave as if the stiff rocks are floating in between soft layers where most of the strain and deformation takes place. This phenomenon was confirmed by examining the maximum strains at the different layers of the sites, which indicated that most of the strains are accommodated at the soft layers, while the basalt layers behave almost rigidly. This is a very important observation that average shear wave velocity of a site is a poor indicator of its dynamic characteristics when the site consists of sharp impedance contrasts, like in the study area where soft layers are sandwiched between stiff rock. While $V_{S,30}$ may be a good indicator of dynamic site characteristic when the stiffness of the soil layers increases with depth, its use in volcanic formations having sharp impedance contrasts seems unreliable.

This observation has important practical implications which need to be carefully considered in engineering design. For example, site effects on design seismic action are quantified in terms of $V_{S,30}$ in Eurocode 8 [15]. According to the code, most of the sites listed in Table 2 should be classified as 'Class A', which means that site corrections factors are not applied in elastic design spectra. However, both HVSR and site response analysis indicate that site effects are significant. In particular, it was observed that the amplitudes and frequency contents of bedrock outcropping motion were significantly altered at these sites. Elastic response spectra of bedrock outcropping motion and the motion at the surface of these sites were also observed to be significantly different, implying that the rock response spectra specified in design codes need to be appropriately adjusted to take the site effects into account. It is therefore important that design seismic action on structures constructed in areas similar to the one being studied here should rely on site specific response analysis using geotechnical information of the site, rather than on simplified methods based on $V_{S,30}$. Another practical implication of these observations is that $V_{S,30}$ should not be used as a site parameter in calibrating GMPEs in areas where sharp impedance contrasts in stratigraphy are expected.

Table 2 – Site fundamental frequency obtained by different methods at seven sites in the study area.

Station	$V_{S,30}$ (m/s)	F_0 (Hz)	F_{30} (Hz)	F_e (Hz)	F_i (Hz)
BFC-2	833	0.98	6.94	1.44	0.84
BFC-3	655	1.20	5.46	1.40	0.96
BFC-4	759	1.24	6.32	1.40	0.89
BFP-2	453	1.23	3.78	1.60	0.84
BFP-3	813	1.06	6.77	1.50	1.04
LD-9	1089	1.02	9.08	1.70	0.79
ST-23	963	4.40	8.03	3.40	2.46

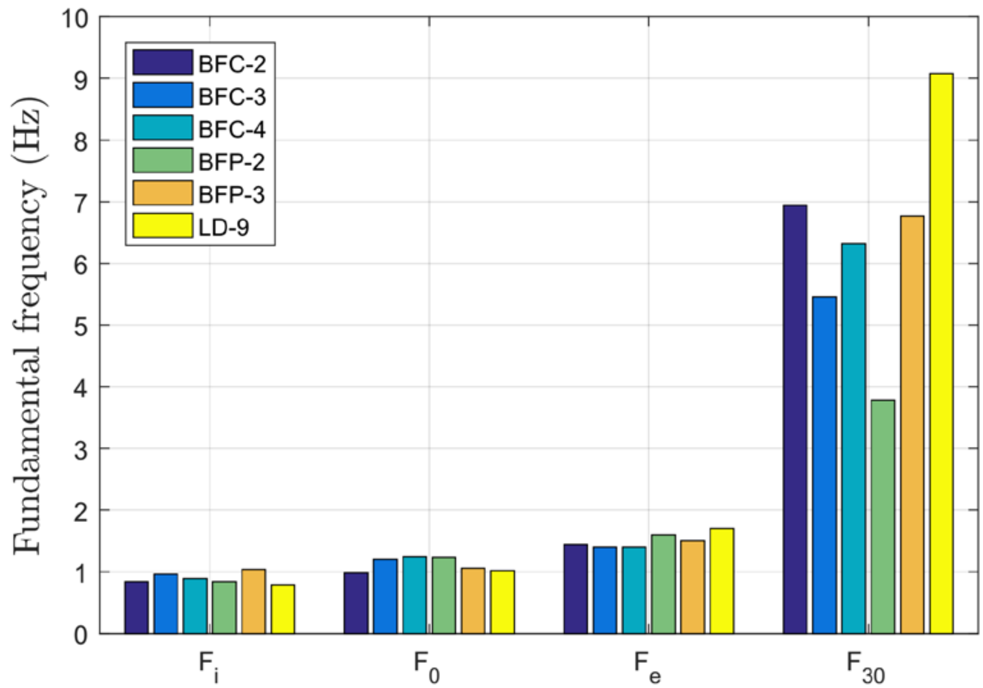

Fig. 9 – Fundamental frequency of different sites obtained from different methods.

7. Conclusions

A detailed analysis of site effects on seismic ground motion in a volcanic environment has been presented. The sites under study consist of layers of very soft sand and tephra/scoria sandwiched between very stiff basalt layers. Such discontinuities in impedance of the different layers was found to result in a site response that was primarily controlled by the properties of the soft layers. Inspection of maximum strain amplitudes at different layers showed that most of the deformation was accommodated by the softer layers, with the basalt layers showing very rigid behaviour. This resulted in much lower site fundamental frequencies than would be implied by average shear wave velocity at the sites. The results indicate that $V_{S,30}$, which is commonly used as a site classification parameter in contemporary seismic design codes and GMPEs, does not represent dynamic characteristics of volcanic formations where sharp impedance contrasts exist. Site effects at such areas should therefore be studied carefully, for example, by performing site response analysis based on local geotechnical information.

Site fundamental frequencies inferred from ambient vibration HVSR curves were found to be fairly consistent with those estimated from elastic transfer functions of the sites computed from geotechnical information provided by borehole data. This reinforces the suitability of using HVSR method in estimating site fundamental frequency. The higher-mode frequencies and amplification factors obtained from HVSR curves were, however, significantly different from those obtained from elastic transfer functions.

8. Acknowledgements

The research presented herein was fiancially supported by the National Power Company of Iceland, Landsvirkjún, and the University of Iceland Research Fund.

9. References

[1] Ingólfsson, Jónas Þ (2015a): *Búrfell Wind Farm Site Investigations:* Geological site investigations with ram sounding, core and percussion drilling and aggregate research. *Technical report, EFLA Consulting Engineers*, Iceland.

[2] Loftsson, M, Steingrímsson, BÓ (2010): Tæknilegir eiginleikar mismunandi berggerða. *Technical report (in Icelandic), Mannvit, Iceland*.

[3] Ingólfsson, JÞ (2015b): Personal communication in a meeting at EFLA Consulting Engineers, Iceland.

[4] Nogoshi M, Igarashi T (1971): On the amplitude characteristics of microtremor (part 2) (in Japanese with English abstract). *Journal of seismological Society of Japan,* **24**, 26–40.

[5] Nakamura Y (1989): A method for dynamic characteristic estimation of subsurface using microtremor on the ground surface. *Q. Rep. Railway Tech. Res. Inst.* **30** (1), 25–33.

[6] Bard, P (2005): SESAME-Team (2005) Guidelines for the implementation of the H/V spectral ratio technique on ambient vibrations: measurements, processing, and interpretations. *Technical report*, *SESAME European research project*.

[7] Onno, K, Ohmachi, T (1998): Ground-motion characteristics estimated from spectral ratio between horizontal and vertical components of microtremor. *Bulletin of the Seismological Society of America*, **88**(1), 228–241.

[8] Schnabel, B, Lysmer, J, Seed, HB (1972): Shake: A Computer Program for Earthquake Response Analysis of Horizontally Layered Sites. *Technical Report No. EERC 72-12,* University of California, Berkeley.

[9] Idriss, IM, Sun, J I (1992): SHAKE91: A computer program for conducting equivalent linear seismic response analyses of horizontally layered soil deposits. *Center for Geotechnical Modeling, Department of Civil and Environmental Engineering,* University of California, Davis, CA.

[10] Seed, HB, Idriss, IM (1970): Soil moduli and damping factors for dynamic response analyses. *Technical Report No. EERC 70-10,* University of California, Berkeley.

[11] Senetakis, K, Anastasiadis, A, Pitilakis, K (2013): Normalized shear modulus reduction and damping ratio curves of quartz sand and rhyolitic crushed rock. *Soils and Foundations,***53**(6), 879–893.

[12] Sigurðsson, G Ö (2015) Seismic response of wind turbine structures in the near-fault region. *MSc. Thesis, University of Iceland,* Iceland.

[13] Rupakhety, R, Sigurdsson, S U, Papageorgiou, A S, Sigbjörnsson, R (2011). Quantification of ground-motion parameters and response spectra in the near-fault region. *Bulletin of Earthquake Engineering*, **9**(4), 893–930.

[14] Ambraseys, N N, Smit, P, Douglas J, Margaris, B, Sigbjörnsson, R, Ólafsson, S, Suhadolc, P, Costa, G (2004): Internet Site for European strong-motion data. *Bolletino di Geofisica Teorica ed Applicata*, **45**(3):113–129

[15] Rupakhety R, Ólafsson S, Sigurðsson GÖ, Sigbjörnsson R (2016): Site-specific seismic hazard assessment including near-fault and local site effects for the proposed windfarm in the Búrfellslundur area in South Iceland. *Technical Report LV-2014-040*, National Power Company of Iceland report.

[16] CEN (2004): Eurocode 8: Design of Structures for Earthquake Resistance—Part 1: General Rules. Seismic Actions and Rules for Buildings. *Comité Européen de Normalisation*.

[17] UBC, Uniform Building Code (1997). Uniform building code. *Int. Conf. Building Officials*.